Polymer Chemistry

Accepted Manuscript

ROYAL SOCIETY OF CHEMISTRY

www.rsc.org/polymers

Polymer Chemistry

RSCPublishing

ARTICLE

π-Conjugated Polymers Derived from 2,5-Bis(2-decyltetradecyl)-3,6-di(selenophen-2-yl)pyrrolo[3,4-c]pyrrole-1,4(2H,5H)-dione for High-Performance Thin Film Transistors

Cite this: DOI: 10.1039/x0xx00000x

Received ooth January 2012,
Accepted ooth January 2012

DOI: 10.1039/x0xx00000x

www.rsc.org/

Tae Wan Lee, Dae Hee Lee, Jicheol Shin, Min Ju Cho, and Dong Hoon Choi*

Novel 2,5-bis(2-decyltetradecyl)-3,6-di(selenophen-2-yl)pyrrolo[3,4-*c*]pyrrole-1,4(2*H*,5*H*)-dione (DSDPP)-containing conjugated polymers with different donor monomers were synthesized via Pd(0)-catalyzed Stille coupling reaction. Solubilized 2-decyltetradecyl (DT) groups were tethered to the N-atoms in diketopyrrolopyrrole (DPP). As electron-donating units, bithiophene (BT) and π-extended (*E*)-2-(2-(thiophen-2-yl)vinyl)thiophene (TVT) were introduced into the polymer backbone. Besides thiophene-based monomers, biselenophene (BS) and (*E*)-2-(2-(selenophen-2-yl)vinyl)selenophene (SVS) were also copolymerized with the same DSDPP-based monomer. DSDPP-BS and DSDPP-SVS copolymers exhibited higher hole mobility in thin film transistor (TFT) than the corresponding BT and TVT analogs. In particular, a TFT having a DSDPP-SVS copolymer-based active layer showed the highest hole mobility of ~5.23 $cm^2\ V^{-1}\ s^{-1}$ and high current on/off ratios of ~10^7; this indicates that the π-extended SVS significantly improves the charge transport properties.

Introduction

High performance organic field-effect transistors (OFETs) have been fabricated from soluble semiconducting π-conjugated polymers owing to their high mechanical robustness required for flexible, low-cost devices.[1-8] Among various types of semiconducting π-conjugated polymers, those composed of repeating donor (D) and acceptor (A) monomers exhibit intriguingly high performances in solution-processed thin-film transistors (TFTs). The high charge carrier mobility observed in the π-conjugated polymers is mainly attributed to strong intermolecular interactions *via* π–π stacking of the D-A molecular framework leading to a decrease in band gap energies.[9–11] Therefore, low band gap D-A conjugated polymers have been recognized as promising materials both for organic field effect transistors (OFETs)[12] and organic photovoltaic devices (OPVs).[13,14]

Recently, diketopyrrolopyrrole (DPP) has been frequently employed as an acceptor unit in high-performance polymers for TFTs and OPVs, because of its strong electron affinity and symmetric fused-ring structure, which imposes coplanarity and promote intermolecular interaction.[15-17] Several DPP-based conjugated polymers incorporating various electron-donating moieties such as thiophene,[18] quarterthiophene,[19,20] (*E*)-2-(2-(thiophen-2-yl)vinyl)thiophene,[10,21] benzene,[22] dithienopyrrole,[23–25] thieno[3,2-*b*]thiophene,[26,27] biselenophene,[28] (*E*)-2-(2-(selenophen-2-yl)vinyl)selenophene,[21,29] and benzothiadiazole[30] have shown high unipolar or ambipolar FET characteristics. Besides the popular thiophene-based donor monomers, the more electron-rich selenophene-based monomers have also attracted much interest for developing high-performance semiconducting polymers for TFTs.[31–33] In addition, thiophene,[34] furan,[35] thienothiophene[36] and phenyl[37] units were mainly anchored into 3,6-position of pyrrolopyrrole-dione in the structure of DPP-based acceptor monomer and the copolymers bearing above mentioned four monomers have recently been reported.

Copolymerization of a thiophene donors with thieno[3,2-*b*]thiophene-diketopyrrolopyrrole-based monomer acceptors was recently reported by Bronstein *et al.* These new copolymers exhibited hole mobility as high as 1.95 $cm^2\ V^{-1}\ s^{-1}$.[36(a)] Another copolymer, DPPT-TT containing di(thienyl)-DPP acceptor and thieno[3,2-*b*]thiophene donor units displayed well-balanced ambipolar performance with high hole and electron mobility (both >1 $cm^2\ V^{-1}\ s^{-1}$).[38] Heeney *et al.* synthesized a polymer containing 2,5-bis(2-octyldodecyl)-3,6-di(selenophen-2-yl)pyrrolo[3,4-*c*]pyrrole-1,4(2*H*,5*H*)-dione and thieno[3,2-*b*]thiophene, which also exhibited ambipolar charge transport in OFETs. High and balanced electron and hole mobilities (>0.1 $cm^2\ V^{-1}\ s^{-1}$) were observed at room temperature under nitrogen. They also reported that the

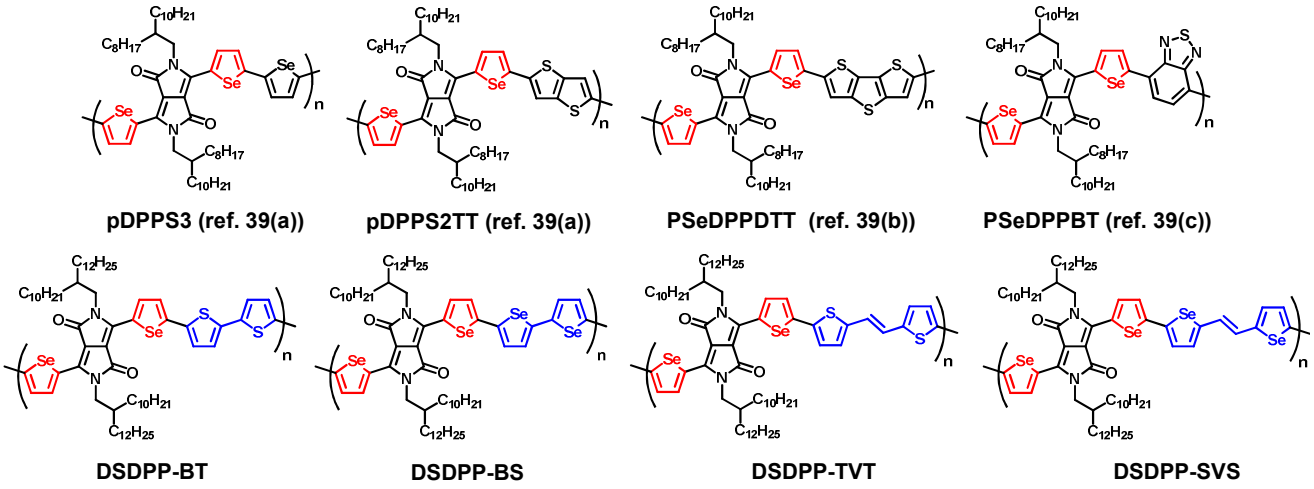

Fig. 1 Chemical structures of DSDPP-containing polymers reported in the literature[39] (top) and synthesized in this study (bottom).

selenophene-DPP-based and benzothiadiazole-based copolymers exhibited high and balanced electron and hole mobilities up to 0.8 $cm^2\ V^{-1}\ s^{-1}$ in bottom- and top-gate TFT devices after thermal annealing.[39] However, little attention was paid to the DPP-based conjugated polymers bearing 2,5-bis(2-octyldodecyl)-3,6-di(selenophen-2-yl)pyrrolo[3,4-*c*]pyrrole-1,4(2*H*,5*H*)-dione) compared to the polymers bearing 2,5-bis(2-octyldodecyl)-3,6-di(thiophen-2-yl)pyrrolo[3,4-*c*]pyrrole-1,4(2*H*,5*H*)-dione. Moreover, no polymer composed of 2,5-bis(2-decyltetradecyl)-3,6-di(selenophen-2-yl)pyrrolo[3,4-*c*]pyrrole-1,4(2*H*,5*H*)-dione) (DSDPP) and selenophene-based donor monomers has been reported yet, to the best of my knowledge.

Herein we describe the synthesis of a new series of conjugated polymers containing DSDPP electron acceptor. Four electron-donating monomer units, bithiophene (BT), (*E*)-2-(2-(thiophen-2-yl)vinyl)thiophene (TVT), biselenophene (BS), and (*E*)-2-(2-(selenophen-2-yl)vinyl)selenophene (SVS) were copolymerized with DSDPP to form low band gap copolymers. The solubility of the four polymers was substantially improved by introducing 2-decyltetradecyl (DT) groups at the N-atoms of the DPP unit. The copolymers containing BS and SVS donor monomers have lower band gaps than those having thiophene-based donor units. Because selenium is more polarizable than sulfur, the stronger interchain Se•••Se interactions are expected to improve the charge transport property in solid states.[40] Accordingly, the four DSDPP-containing polymers showed a high hole mobility in the range of 0.72 ~ 5.23 $cm^2\ V^{-1}\ s^{-1}$ in TFT devices. In particular, among the four different DSDPP-based polymers, the TFTs bearing an active channel layer made of DSDPP-SVS copolymer showed the highest hole mobility of ~5.23 $cm^2\ V^{-1}\ s^{-1}$ with a moderately high current on/off ratio ($I_{on/off}$ ~10^7).

Experimental

Materials and Synthesis: All reagents were purchased from Sigma-Aldrich, TCI, and Acros Co. and used without further purification, unless stated otherwise. Reagent grade solvents used in this study were freshly dried under standard distillation methods. 3,6-Bis-(selenophenyl)-1,4-diketopyrrolo[3,4-*c*]pyrrole,[39(a)] 2-decyltetradecyl iodide,[36(b)] 5,5'-bis(trimethylstannyl)-2,2'-bithiophene,[28] 5,5'-bis(trimethylstannyl)-2,2'-biselenophene,[28] 1,2-(*E*)-bis(5-(trimethylstannyl)thiophen-2-yl)ethene[41] and 1,2-(*E*)-bis(5-(trimethylstannyl)selenophen-2-yl)ethene[29] were synthesized by following the literature methods.

2,5-Di(2-decyltetradecyl)-3,6-bis-(selenophenyl)-1,4-diketopyrrolo[3,4-*c*]pyrrole (2)

2-Decyltetradecyl iodide (13.67 g, 29.4 mmol) was added to a mixture of 3,6-bis-(selenophenyl)-1,4-diketopyrrolo[3,4-*c*]pyrrole, (**1**; 2.9 g, 7.36 mmol), K_2CO_3 (4.57 g, 33.1 mmol), and 18-crown-6 (~20 mg) in dry DMF (60 mL) at 120 °C. After stirring 18 h, the reaction mixture was cooled, poured into ice-water (200 mL), and extracted with $CHCl_3$ (3 × 100 mL). The combined organic extracts were washed with water and brine, and dried over Na_2SO_4. The solvent was then removed under reduced pressure and the crude product was purified by column chromatography on silica (eluent: CH_2Cl_2/hexane = 1:1) to give compound **2** as a purple-red solid (2.0 g, 25%).
^{1}H NMR (400 MHz, $CDCl_3$) δ (ppm): 8.82 (d, *J*=4.4 Hz, 2H), 8.38 (d, *J*=5.6 Hz, 2H), 7.49 (m, 2H), 3.97 (d, *J*=7.2 Hz, 4H), 1.91 (br, 2H), 1.21 (m, 80H), 0.87 (m, 12H). ^{13}C NMR (100 MHz, $CDCl_3$): 161.84, 142.15, 136.93, 136.47, 134.02, 130.69, 108.00, 46.11, 37.65, 31.92, 31.91, 31.19, 30.00, 29.69, 29.67, 29.64, 29.62, 29.55, 29.36, 29.35, 26.19, 22.69, 14.12. HRMS (m/z, MALDI-TOF) Calcd. for $C_{62}H_{104}N_2O_2Se_2$ 1068.6428, found 1068.4841; Anal. Calcd for $C_{62}H_{104}N_2O_2Se_2$: C, 69.76; H, 9.82; N, 2.62. Found: C, 69.51; H, 9.57; N, 2.76.

2,5-Di(2-decyltetradecyl)-3,6-bis-(5-bromo selenophenyl)-1,4-diketopyrrolo[3,4-*c*]pyrrole (3)

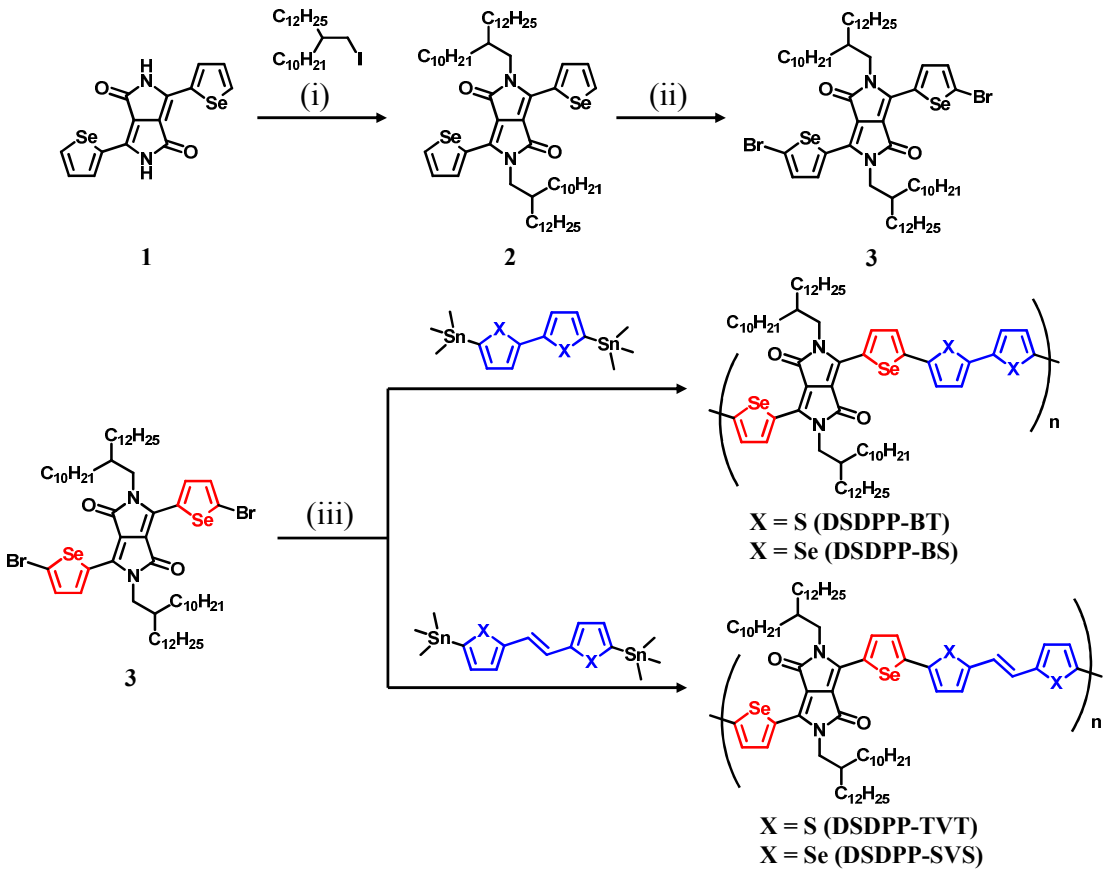

Scheme 1. Synthetic procedures for DSDPP-based polymers. (i) K_2CO_3, 18-crown-6, DMF, 120 °C; (ii) NBS, $CHCl_3$, r.t.; and (iii) $Pd(PPh_3)_4$, toluene, 90 °C.

To a stirred solution of compound **2** (1.07 g, 1.0 mmol) in $CHCl_3$ (40 mL) under argon atmosphere, N-bromosuccinimide (NBS, 0.39 g, 2.2 mmol) was added in small portions. Then, the reaction mixture was protected from light and stirred at room temperature overnight. After completion of the reaction, the reaction mixture was poured into methanol (300 mL). The resulting precipitate was filtered and washed with hot distilled water and methanol. The crude product was further purified by column chromatography on silica (eluent: CH_2Cl_2/hexane = 2:3) to obtain compound **3** as a dark purple solid (0.85 g, 88%). ^{1}H NMR (400 MHz, $CDCl_3$), δ (ppm): 8.40 (d, J=4.8 Hz, 2H), 7.40 (d, J=4.0 Hz, 2H), 3.88 (d, J=7.6 Hz, 2H), 1.88 (br, 2H), 1.21 (m, 80H), 0.88 (m, 12H). ^{13}C NMR (100 MHz, $CDCl_3$): 161.53, 140.90, 136.08, 135.62, 134.23, 123.99, 108.26, 46.33, 37.64, 31.94, 31.93, 31.86, 29.99, 29.72, 29.70, 29.66, 29.65, 29.56, 29.39, 29.37, 26.15, 22.71, 14.15. HRMS (m/z, MALDI-TOF) Calcd. for $C_{62}H_{102}Br_2N_2O_2Se_2$ 1224.4638, found 1224.4803; Anal. Calcd for $C_{62}H_{102}Br_2N_2O_2Se_2$: C, 60.78; H, 8.39; N, 2.29. Found: C, 60.43; H, 8.27; N, 2.45.

Synthesis of DSDPP-BT

Compound **3** (200 mg, 0.16 mmol) and 5,5'-bis(trimethylstannyl)-2,2'-bithiophene (80 mg, 0.16 mmol) were dissolved into 15 mL toluene in a Schlenk flask protected by argon. The solution was flushed with argon for 10 minutes followed by addition of $Pd(PPh_3)_4$ (19 mg, 10 mol%), and again flushed with argon for another 10 min. The oil bath was gradually heated to 90 °C, and the reaction mixture was stirred for 72 h at 90 °C under argon atmosphere. Next, the mixture was cooled down to room temperature and the polymer was precipitated into methanol/H_2O (9:1 v/v; 200 mL). The crude polymer was collected by filtration and then purified by Soxhlet extraction with methanol, acetone, hexane, and $CHCl_3$, successively. The polymer was obtained as dark green-purple solid (yield 98%) upon evaporation of the $CHCl_3$ extract and precipitation into methanol. M_n=114.0 kDa; polydispersity=2.41. ^{1}H NMR (400 MHz, $CDCl_3$), δ (ppm): 8.49 (br, 4H), 7.07 (br, 4H), 3.55 (br, 4H), 1.25 (m, 80H), 0.88 (m, 12H). Anal. Calcd for $C_{70}H_{108}N_2O_2S_2Se_2$: C, 68.26; H, 8.84; N, 2.27; S, 5.21. Found: C, 68.12; H, 8.68; N, 2.25; S, 5.35.

Synthesis of DSDPP-TVT

DSDPP-TVT was synthesized with the same method used for DSDPPT-BT, but by using (*E*)-1,2-bis(5-(trimethylstannyl)thiophen-2-yl)ethene instead of 5,5'-bis(trimethylstannyl)-2,2'-bithiophene. The polymer was obtained as dark green-purple solid (yield 98%). M_n=140.7 kDa; polydispersity=2.88. ^{1}H NMR (400 MHz, $CDCl_3$), δ (ppm): 8.55 (br, 4H), 7.11 (br, 6H), 3.52 (br, 4H), 1.27 (m,

80H), 0.88 (m, 12H). Anal. Calcd for $C_{72}H_{110}N_2O_2S_2Se_2$: C, 68.76; H, 8.82; N, 2.23; S, 5.10. Found: C, 68.64; H, 8.77; N, 2.25; S, 5.15.

Synthesis of DSDPP-BS

DSDPP-BS was synthesized with the same method used for DSDPPT-BT, but by using 5,5'-bis(trimethylstannyl)-2,2'-biselenophene instead of 5,5'-bis(trimethylstannyl)-2,2'-bithiophene. The polymer was obtained as dark green-purple solid (yield 97%). M_n=217.3 kDa; polydispersity=3.21. ^{1}H NMR (400 MHz, $CDCl_3$), δ (ppm): 8.52 (br, 4H), 7.19 (br, 4H), 3.54 (br, 4H), 1.25 (m, 80H), 0.88 (m, 12H). Anal. Calcd for $C_{70}H_{108}N_2O_2Se_4$: C, 63.43; H, 8.21; N, 2.11. Found: C, 63.25; H, 8.10; N, 2.15.

Synthesis of DSDPP-SVS

DSDPP-SVS was synthesized with the same method used for DSDPPT-BT, but by using (*E*)-1,2-bis(5-(trimethylstannyl)selenophen-2-yl)ethene instead of 5,5'-bis(trimethylstannyl)-2,2'-bithiophene. The polymer was obtained as dark green-purple solid (yield 98%). ^{1}H NMR (400 MHz, $CDCl_3$), δ (ppm): 8.64 (br, 4H), 7.20 (br, 6H), 3.51 (br, 4H), 1.25 (m, 80H), 0.88 (m, 12H). M_n=347.0 kDa; polydispersity=3.10. Anal. Calcd for $C_{72}H_{110}N_2O_2Se_4$: C, 63.99; H, 8.20; N, 2.07. Found: C, 63.80; H, 8.07; N, 2.12.

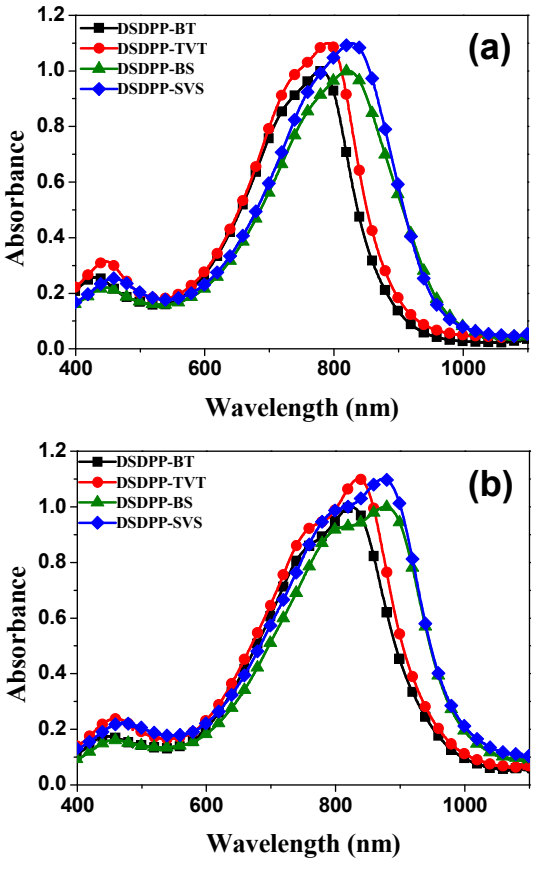

Fig. 2 UV-Vis-NIR absorption spectra of DSDPP-based polymers in solution ($CHCl_3$) (a) and film (b).

Instruments

The ^{1}H NMR spectra were recorded using a Varian Mercury NMR 400 MHz spectrometer (Varian, Palo Alto, CA, USA) in $CDCl_3$ (Cambridge Isotope Laboratories, Inc., Andover, MA, USA). The ^{13}C NMR spectra were recorded using a Varian Inova-500 spectrometer. MALDI-TOF MASS was performed on a Voyager-DE STR workstation by Applied Biosystems. The elemental analyses were performed on an EA1112 (Thermo Electron Corp., West Chester, PA, USA) elemental analyzer. The molecular weights of the polymers were determined by gel permeation chromatography (GPC) (Waters GPC, Waters 515 pump, Waters 410 RI, 2× PLgel Mixed-B) using polystyrene standard and $CHCl_3$ as the eluent (T = 35 °C) at the Korean Polymer Testing and Research Institute, Seoul, Korea.

The thermal properties of the four polymers were studied under a nitrogen atmosphere on a Mettler 821^e differential scanning calorimetry (DSC) (Mettler, Greifensee, Switzerland). Thermal gravimetric analysis (TGA) was performed on a Mettler TGA50 instrument (temperature rate 10 °C min^{-1} under nitrogen). The redox properties of the four polymers were examined by cyclic voltammetry (CV) (EA161 eDAQ). The polymer thin films were coated on a Pt wire using $CHCl_3$. The electrolyte solution was 0.10 M tetrabutylammonium hexafluorophosphate (Bu_4NPF_6) in freshly dried acetonitrile. Ag/AgCl and Pt wire (0.5 mm in diameter) electrodes were used as the reference electrode and the counter electrode, respectively. The scan rate was 20 mV s^{-1}. Grazing incidence X-ray diffraction (GI-XRD) measurements were carried out at the 3C (SAXS I) beam lines (energy = 10.0 keV, pixel size = 79.6 μm, wavelength = 1.165 Å) at the Pohang Accelerator Laboratory (PAL). The diffraction data were obtained in a 2θ scanning interval between 0° and 25°; the components of the scattering vector parallel (q_{xy}) and perpendicular (q_z) to the substrate were determined using the following equation: $q = (4\pi/\lambda)\sin\theta$, where θ is the half scattering angle and λ is the wavelength of the incident radiation. The film samples were prepared by spin-coating onto OTS-SiO_2/Si followed by drying at 50 °C under vacuum. Atomic Force Microscopy (AFM) (XE-100 Advanced Scanning Probe Microscope, PSIA) in tapping mode with a silicon cantilever was used to characterize the surface morphologies of the film samples fabricated by spin-casting (1000 rpm) of the polymer solution (2 mg mL^{-1} in $CHCl_3$) on silicon wafers followed by drying at 50 °C in vacuum.

In order to study the UV-visible-NIR absorption behavior, the thin film samples of the four polymers were fabricated on glass substrates as follows. A solution (0.5 wt% in $CHCl_3$) of each polymer was filtered through an Acrodisc syringe filter (Millipore 0.45 μm, Millipore, Billerica, MA, USA) and subsequently spin-cast on glass. The thin films were dried at 50 °C for 2 h in vacuum. The absorption spectra of the samples as thin films and as solutions (1×10^{-5} mol L^{-1} in $CHCl_3$) were recorded on a HP 8453 photodiode array UV-Vis-NIR absorption spectrometer in the 190–1100 nm range.

Fabrication of Organic Thin Film Transistors

For characterization of TFT performances, the bottom-gate bottom-contact (BGBC) device geometry was employed. The OTFT devices were fabricated on 300 nm n-doped Si/SiO_2 substrates, where n-doped Si and SiO_2 were used as the gate electrode and gate dielectric, respectively. The substrate was cleaned with acetone, cleaning agent, deionized water, and isopropanol in an ultrasonic bath. The cleaned substrates were dried in vacuum at 120 °C for 1 h, and then treated with UV/ozone for 20 min. Before the electrodes deposition, the SiO_2 gate dielectrics were treated with OTS to form a hydrophobic surface of SiO_2/Si. The source and drain electrodes were prepared using thermal evaporation of gold (70 nm) through a shadow mask with a channel width of 1500 μm and a length of 100 μm. Finally, the polymer layer was deposited on the OTS-treated substrates by spin-casting (2000 rpm for 30 s) from a solution (2 mg mL^{-1} in $CHCl_3$) in ambient conditions. For annealing thin film, the TFT devices were placed on a hotplate in air at a fixed temperature for 10 min. Field-effect current-voltage characteristics of the devices were determined in air on a Keithley 4200 SCS semiconductor parameter analyzer. The field effect mobilities were extracted in the saturation regime using the relationship $\mu_{sat}=(2I_{DS}L)/(WC_i(V_G-V_{TH})^2)$, where I_{DS} is the saturation drain current, C_i is the capacitance (~11.5 nF cm^{-2}) of SiO_2 dielectric, V_G is the gate bias, and V_{TH} is threshold voltage. Mobility data were averaged from measurements of more than 15 different devices.

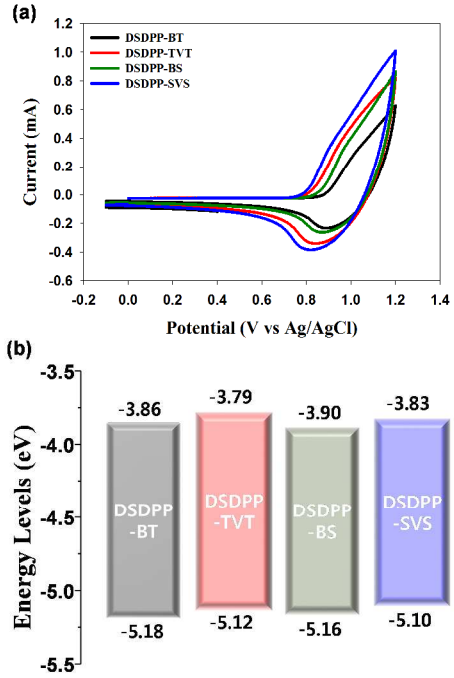

Fig. 3 (a) Cyclic voltammograms and (b) HOMO and LUMO energy levels of the four DSDPP-based polymers.

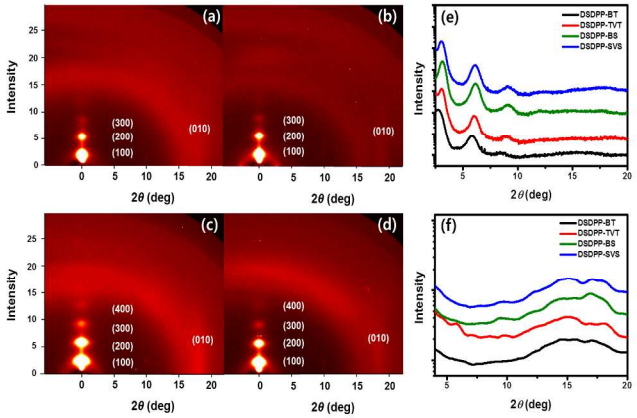

Fig. 4 2D GI-XRD patterns of DSDPP-based polymer films annealed at 200 °C: (a) DSDPP-BT, (b) DSDPP-TVT, (c) DSDPP-BS, and (d) DSDPP-SVS. (e) out-of-plane profiles, (f) in-plane profiles.

Results and discussion

Synthesis and Characterization

Synthetic procedures of DSDPP monomer and four different DSDPP-based polymers are shown in Scheme 1. Compound **1** was synthesized according to the reported literature method.[39(a)] The branched, long-chain DT group was attached to the N-atoms in **1** to ensure good polymer solubility. Bromination of the resulting compound **2** with N-bromosuccinimide (NBS) under argon atmosphere yielded the DSDPP-monomer **3**. Four

Table 1. Physical, Optical, and Electrochemical Properties of the DSDPP-Based Polymers

polymers	M_n [a] (kDa)	PDI	T_d (°C)	λ_{max} (nm)		E_g^{opt} [b] (eV)	E_{ox}^{onset} (V)	HOMO [c] (eV)	LUMO [d] (eV)
				solution	film				
DSDPP-BT	114.0	2.41	402	780	824	1.32	0.88	-5.18	-3.86
DSDPP-TVT	140.7	2.88	400	790	837	1.33	0.82	-5.12	-3.79
DSDPP-BS	217.3	3.21	397	821	877	1.26	0.86	-5.16	-3.90
DSDPP-SVS	347.0	3.10	386	828	873	1.27	0.80	-5.10	-3.83

[a] Determined by GPC and reported as their polystyrene equivalents. [b] Calculated from the onset of the optical absorption. [c] Determined by CVs of thin films on Pt electrode. [d] LUMO = E_g^{opt} + HOMO.

donor monomeric units, BT, TVT, BS, and SVS, were copolymerized with the acceptor monomer DSDPP *via* Stille coupling. The DSDPP-based polymers were purified by precipitation into methanol followed by Soxhlet extraction to remove low-molecular weight materials and catalyst residues using acetone, hexane, and $CHCl_3$, successively. The $CHCl_3$ fraction was concentrated in volume and the pure polymers were collected by precipitation in methanol in quantitative yields. The structures of the polymers (DSDPP-BT, DSDPP-TVT, DSDPP-BS, and DSDPP-SVS) were deliberately selected to explore the effect of selenophene and conjugation length on the physical, optical, and molecular electronic properties.

The gel permeation chromatography (GPC) measurements provided high number-averaged molecular weights (M_n) of 114.0, 140.7, 217.3, and 347.0 kDa for DSDPP-BT, DSDPP-TVT, DSDPP-BS, and DSDPP-SVS, respectively. The polydispersity indices were in the range of 2.4−3.2 (Fig. S1-S4). These polymers displayed good solubility in chloroform.

The four polymers showed excellent thermal stability up to 380 °C under nitrogen by thermogravimetric analysis (TGA). (see Fig. S5) Differential scanning calorimetry (DSC) measurements at a heating/cooling rate of 10 °C min^{-1} under nitrogen showed melting behaviors at 297, 310, 334 and 331 °C, for DSDPP-BT, DSDPP-TVT, DSDPP-BS, and DSDPP-SVS, respectively. (see Fig. S6)

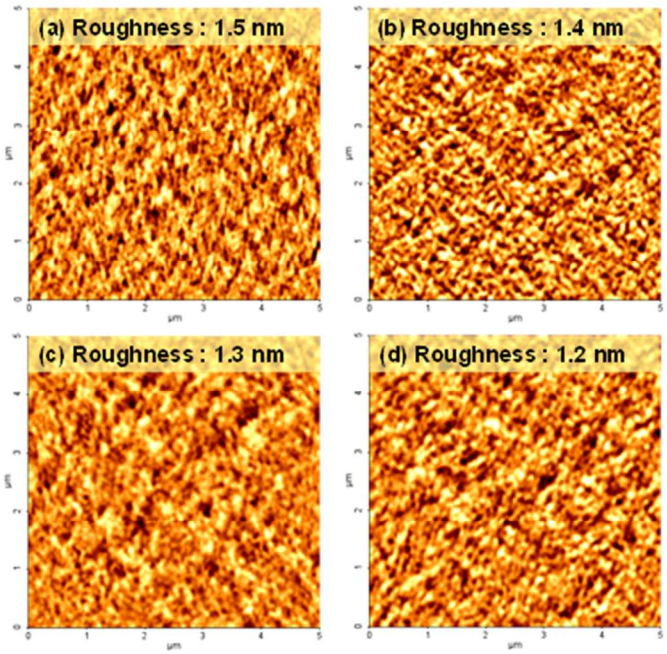

Fig. 5 AFM images of heights (a) DSDPP-BT, (b) DSDPP-TVT, (c) DSDPP-BS, and (d) DSDPP-SVS polymers thin films (5 × 5 μm), thermally annealed at 200 °C.

Optical Absorption, Electrochemical Properties

Fig. 2 shows the absorption spectra of DSDPP-BT, DSDPP-TVT, DSDPP-BS, and DSDPP-SVS in solution ($CHCl_3$) and films. The maximum absorption wavelength (λ_{max}) and the optical band gap (E_g^{opt}) are summarized in Table 1. All four polymers exhibit weak absorption bands at 400–500 nm, and low energy, intense absorption bands at 600–1000 nm. The latter can be assigned to the intramolecular charge transfer (ICT) between D and A units in the polymer backbones. The absorption in $CHCl_3$ solutions further expands into near-infrared, with λ_{max} at 780, 790, 821, and 828 nm for DSDPP-BT, DSDPP-TVT, DSDPP-BS, and DSDPP-SVS, respectively. Compared to the solution spectra, the spectra in thin films are broader and red-shifted by 45–56 nm, which is common for crystalline conjugated polymers owing to intermolecular interactions in the film state. Although the four polymers contain the DSDPP acceptor monomer, DSDPP-BS and DSDPP-SVS exhibit red shifts compared to DSDPP-BT and DSDPP-TVT. This is attributed to the stronger donating ability of selenophene unit accompanying with more quinoidal nature.

The optical band gaps (E_g^{opt}) are 1.32 eV for DSDPP-BT, 1.33 eV for DSDPP-TVT, 1.26 eV for DSDPP-BS, and 1.27 eV for DSDPP-SVS, as determined from the absorption peak edges in the thin film spectra. Thus, DSDPP-BS and DSDPP-SVS are characterized by smaller band gaps than those of DSDPP-BT and DSDPP-TVT.

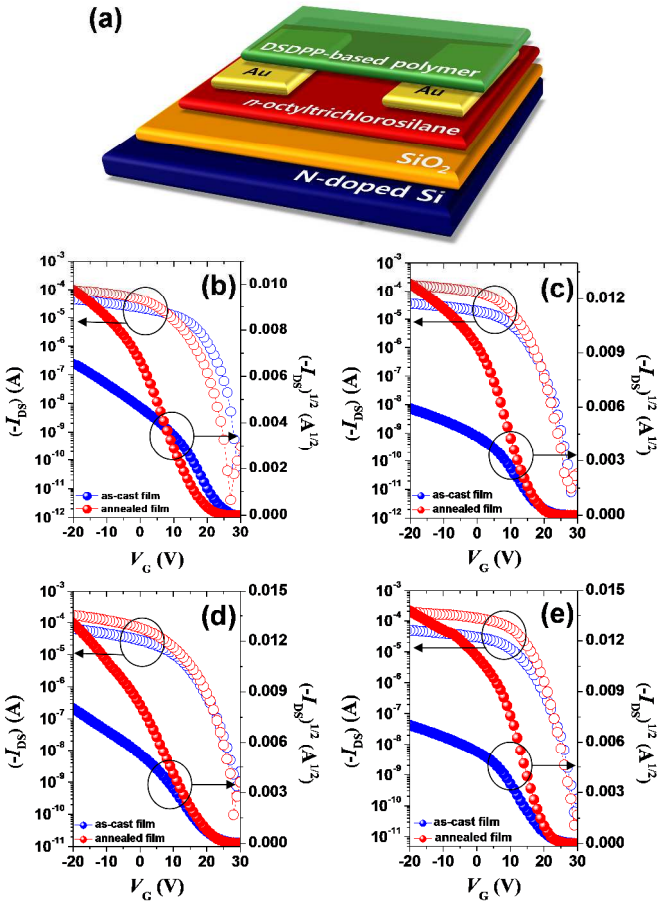

Fig. 6 (a) Schematic illustration of OTFT in BGBC configuration and (b-e) transfer characteristics of TFT devices incorporating (b) DSDPP-BT, (c) DSDPP-TVT, (d) DSDPP-BS, and (e): DSDPP-SVS as-cast and annealed at 200 °C films at V_{DS}= –100 V (L = 100 μm, W = 1500 μm).

The highest occupied molecular orbital (HOMO) levels of the four polymers in thin films were characterized by CV in 0.1 M Bu_4NPF_6 solutions in dry acetonitrile. The cyclic voltammograms (see Fig. 3a) indicate a reversible oxidation behavior. The HOMO levels calculated by the onset of the oxidation potential are –5.18, –5.12, –5.16, and –5.10 eV for DSDPP-BT, DSDPP-TVT, DSDPP-BS, and DSDPP-SVS, respectively. These results demonstrate that the replacement of thiophene by selenophene increases the electron donating ability, narrows the band gap, and lowers the oxidation potential in agreement with the previous theoretical studies.[42] The LUMO levels were determined from the optical band gap and the HOMO levels (see Fig. 3b). The lower-lying LUMOs of the selenophene donor results in an overall lowering of the LUMO of the polymers containing BS and SVS compared to the polymers bearing BT and TVT. This result is consistent with the HOMO and LUMO energies determined by Density Functional Theory (DFT) calculations (Spartan' 10 program) at the B3LYP/6-31G* level for the geometry-optimized structures of simplified repeating units in DSDPP polymers (see Fig. S7).

Thin Film Microstructure and Morphology

To investigate the influence of the thin film microstructure and surface topographies of the four DSDPP-based polymers on the OTFT performance, the GI-XRD patterns (Fig. 4 and S8) and AFM height images (Fig. 5 and S9) of thin films before and after annealing at 200 °C were characterized. The annealed thin films of DSDPP polymers deposited on OTS-modified SiO_2/Si substrates exhibited a primary diffraction peak at 2θ = 2.80–3.08°, corresponding to $d_{(100)}$-spacing values of 21.7–23.8 Å. The (h00) diffraction peaks for the thermally annealed films become relatively more intense, and well-resolved high-order diffraction peaks are observed. (Fig. 4(e)) Although DSDPP-BT showed less resolved diffraction peaks, the (010) diffraction peaks in the in-plane profiles of the four polymers were observed at around 2θ=16.9~18.0°. (Fig. 4(f)) At the same time, the (200) diffraction peaks almost disappeared, which indicates that the polymer chain arrangement somewhat changed to edge-on manner on the substrate compared to as-spun films. In particular, the π–π stacking distances of DSDPP-TVT and DSDPP-SVS could be obtained to be 3.72 and 3.74 Å, respectively, which are smaller than those of DSDPP-BT and DSDPP-BS ($d_{(010)}$= 3.94 and 3.96 Å, respectively). Therefore, DSDPP-TVT and DSDPP-SVS bearing more π-extended donor moieties could be expected to display more facile charge transport than DSDPP-BT and DSDPP-BS.

The thin film morphologies of the DSDPP-based polymers were investigated using tapping-mode AFM. The as-cast films of the four polymers display highly dense surface morphology with small, connected crystallites having good coverage on the surface. In particular, they form dense fibrillar networks with average surface roughness of 3.1–3.5 nm (see Fig. S9). Highly resolved fibrillar structures are suppressed in the overall surface morphology and the surface roughness is reduced significantly to 1.2–1.4 nm when annealing the films (see Fig. 5). Therefore, it can be conjectured that the internal morphologies of annealed films become more compact and denser than those of as-cast films. The connectivity between neighboring crystallite domains becomes highly developed after thermal annealing, which facilitates building efficient pathways for charge transport thereby enhancing the charge mobility in the OTFT device.[12(a)]

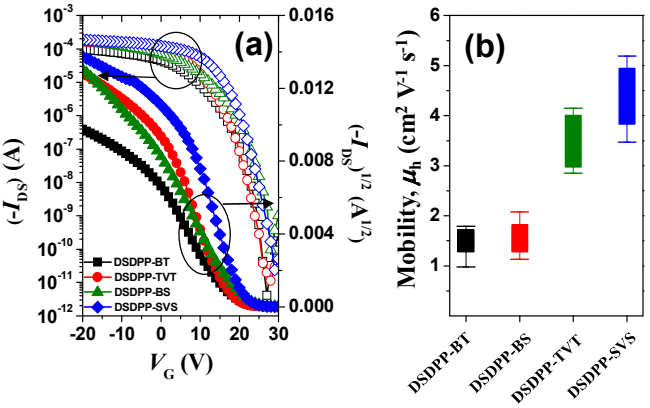

Fig. 7 (a) Transfer curves of TFT devices fabricated from the four DSDPP-based polymers by spin-coating chloroform solutions (2 mg mL^{-1} in $CHCl_3$ at V_{DS}= –100 V; L = 100 μm, W = 1500 μm) after thermal annealing at 200 °C. (b) Comparison of hole mobilities of the four polymers after thermal annealing under ambient conditions.

Electrical Properties of OTFTs Based on DSDPP-Copolymers

The electrical properties of four DSDPP-based copolymers were investigated by fabricating OTFT devices in BGBC configuration (see Fig. 6a) using gold source and drain electrodes by thermal evaporation through a shadow mask. An

Table 2. TFT Device Performance of Solution-Processed, DSDPP-Based Copolymers.

polymers	$T_{annealing}$ (°C)	μ_{max} [a] (cm^2 V^{-1} s^{-1})	I_{on}/I_{off}	V_{TH} (V)
DSDPP-BT	As-cast	0.72 (0.52)[b]	$>10^6$	22
	200	1.79 (1.56)[b]	$>10^7$	19
DSDPP-TVT	As-cast	0.83 (0.76)[b]	$>10^6$	19
	200	4.15 (3.89)[b]	$>10^7$	16
DSDPP-BS	As-cast	0.86 (0.80)[b]	$>10^5$	22
	200	2.08 (1.81)[b]	$>10^6$	19
DSDPP-SVS	As-cast	1.11 (0.97)[b]	$>10^6$	21
	200	5.23 (4.91)[b]	$>10^7$	21

[a] Gate voltage ranges for determining the saturated mobilities: (i) 12 V to 22 V for DSDPP-BT film before annealing; 2 V to 12 V for annealed DSDPP-BTT film. (ii) 8 V to 18 V for DSDPP-TVT film before annealing; 3 V to 14 V for annealed DSDPP-TVT film. (iii) 8 V to 18 V for DSDPP-BS film before annealing; 0 V to 14 V for annealed DSDPP-BS film. (i) 8 V to 18 V for DSDPP-SVS film before annealing; 8 V to 20 V for annealed DSDPP-SVS film. [b] Average value.

n-doped Si/SiO_2 substrate was used as the gate electrode, and an OTS-treated SiO_2 surface layer was used as the gate dielectric insulator. The device performance was measured under ambient conditions. The mobility and threshold voltage were calculated from the saturation regimes. The performance of TFT incorporating the four DSDPP-based polymer thin films before and after annealing at 200 °C is summarized in Table 2; the representative transfer characteristics and output characteristics are shown in Fig. 6b-e and Fig. S10-S11, respectively.

The mobility of as-cast DSDPP-BT thin film is 0.72 cm^2 V^{-1} s^{-1} and, reasonably increases to 1.79 cm^2 V^{-1} s^{-1} with high on/off ratio of 10^{7-8} after thermal annealing at 200 °C. In the case of DSDPP-TVT bearing a π-extended donor moiety, the mobilities are 0.83 cm^2 V^{-1} s^{-1} for the as-cast film and 4.15 cm^2 V^{-1} s^{-1} (with a high on/off ratio of 10^{7-8}) after thermal annealing at 200 °C. The π-extended TVT units incorporated between the DSDPP units in the main chain significantly improve the co-planarity and intermolecular π–π stacking of the polymer backbone, resulting in enhancement in carrier mobility. In addition, the intermolecular interaction between the electron-donating TVT and electron-accepting DPP can further shorten the distances between the polymer chains, which facilitates charge carrier transport.[10]

The mobility of the as-cast DSDPP-BS thin film is 0.86 cm^2 V^{-1} s^{-1}, and it significantly increases to 2.08 cm^2 V^{-1} s^{-1} upon thermal annealing at 200 °C. In contrast, the TFT made of as-cast DSDPP-SVS thin film exhibits an unusually high mobility of 1.11 cm^2 V^{-1} s^{-1} for a pristine polymer film. More impressively, the thermally annealed film of DSDPP-SVS exhibited ~5.23 cm^2 V^{-1} s^{-1}, ($I_{on/off}$ >10^7) which is the highest value among the values obtained from the four polymers. Clearly, the more π-extended structure and the replacement of thiophene with selenophene indeed improves hole transport, presumably due to the stronger intermolecular interaction of selenophene and DPP units combined with a high degree of crystallinity.[42]

In brief, Fig. 7 shows a comparison of the charge transport properties of the four polymers after thermal annealing. The considerably higher hole mobilities (Fig. 7b) of the BS- and SVS-containing copolymers compared to those of BT- and TVT-containing analogs can be clearly recognized from the transfer curves (Fig. 7a). Moreover, TFT devices incorporating the four DSDPP-based copolymers also have an excellent operating cyclic stability in air, maintaining on- and off-current upon continuous switching over 300 cycles (see Fig. S12),

Conclusions

We have synthesized and characterized a new series of conjugated polymers containing DSDPP which has selenophene instead of thiophene flanking an electron-accepting DPP core. BT, TVT, BS, and SVS were selected as electron-donating units. Maintaining a virtually identical conjugation length, the two polymer having selenophene donor units exhibited considerably better charge transport properties as evidenced by the considerably higher carrier mobility in the TFT devices. The hole mobilities of the two copolymers incorporating π-extended donor monomers (TVT and SVS) into the polymer backbone are also higher than the analogous BT- and BS-derived co-polymers. In particular, among the four different DSDPP-based polymers, the TFT device incorporating DSDPP-SVS showed the highest hole mobility of ~5.23 cm^2 V^{-1} s^{-1} with high current on/off ratios of >10^7. Our results unambiguously illustrate the effect of selenophene on charge transport in conjugated polymer TFTs. These high levels of performance demonstrate the strong potential of the DSDPP-SVS copolymer for future application in organic electronic devices.

Acknowledgements

The authors acknowledge the financial support from the Basic Science Research Program through the National Research Foundation (NRF) funded by the Ministry of Education (NRF2012R1A2A1A01008797 and NRF20100020209). D. H. Choi also thanks Prof. J. H. Cho in Sungkyunkwan University for his valuable discussion.

Notes and references

[a] Department of Chemistry, Research Institute for Natural Sciences, Korea University, 5 Anam-dong, Sungbuk-gu, Seoul 136-701, South Korea. E-mail: dhchoi8803@korea.ac.kr.

† Electronic Supplementary Information (ESI) available: GPC, TGA, DSC, theoretical calculations, GI-XRD, AFM image and additional characteristics of OTFTs. See DOI: 10.1039/b000000x/

1 H. Yan, Z. Chen, Y. Zheng, C. Newman, J. R. Quinn, F. Dötz, M. Kastler and A. Facchetti, *Nature*, 2009, **457**, 679.
2 I. McCulloch, M. Heeney, C. Bailey, K. Genevicius, I. Mac-donald, M. Shkunov, D. Sparrowe, S. Tierney, R. Wagner, W. Zhang, M. L. Chabinyc, R. J. Kline, M. D. McGehee and M. F. Toney, *Nat. Mater.*, 2006, **5**, 328.
3 A. S. Dhoot, J. D. Yuen, M. Heeney, I. McCulloch, D. Moses and A. J. Heeger, *Proc. Natl. Acad. Sci. U.S.A.*, 2006, **103**, 11834.
4 H. Pan, Y. Li, Y. Wu, P. Liu, B. S. Ong, S. Zhu, and G. Xu, *J. Am. Chem. Soc.*, 2007, **129**, 4112.
5 D. H. Lee, J. Shin, M. J. Cho, and D. H. Choi, *Chem. Commun.*, 2013, **49**, 3896.
6 J. Lee, A.-R. Han, J. Hong, J. H. Seo, J. H. Oh and C. Yang, *Adv. Funct. Mater.*, 2012, **22**, 4128.
7 M. J. Cho, J. Shin, S. H. Yoon, T. W. Lee, M. Kaur and D. H. Choi, *Chem. Commun.*, 2013, **49**, 7132.
8 M. Kaur, D. S. Yang, J. Shin, T. W. Lee, K. Choi, M. J. Cho and D. H. Choi, *Chem. Commun.*, 2013, **49**, 5495.
9 H. N. Tsao, D. M. Cho, I. Park, M. R. Hansen, A. Mavrinskiy, D. Y. Yoon, R. Graf, W. Pisula, H. W. Spiess and K. Müllen, *J. Am. Chem. Soc.*, 2011, **133**, 2605.
10 H. Chen, Y. Guo, G. Yu, Y. Zhao, J. Zhang, D. Gao, H. Liu and Y. Liu, *Adv. Mater.*, 2012, **24**, 4618.

11 W. Zhang, J. Smith, S. E. Watkins, R. Gysel, M. McGehee, A. Salleo, J. Kirkpatrick, S. Ashraf, T. Anthopoulos, M. Heeney and I. McCulloch, *J. Am. Chem. Soc.*, 2010, **132**, 11437.

12 (a) I. Osaka, G. Sauvé, R. Zhang, T. Kowalewski and R. D. McCullough, *Adv. Mater.*, 2007, **19**, 4160; (b) M. Zhang, H. N. Tsao, W. Pisula, C. Yang, A. K. Mishra and K. Müllen, *J. Am. Chem. Soc.*, 2007, **129**, 3472.

13 (a) D. Mühlbacher, M. Scharber, M. Morana, Z. Zhu, D. Waller, R. Gaudiana and C. Brabec, *Adv. Mater.*, 2006, **18**, 2884; (b) N. Blouin, A. Michaud, D. Gendron, S. Wakim, E. Blair, R. Neagu-Plesu, M. Belletête, G. Durocher, Y. Tao and M. Leclerc, *J. Am. Chem. Soc.*, 2008, **130**, 732.

14 J. Li, K.-H. Ong, S.-L. Lim, G.-M. Ng, H.-S. Tan and Z.-K. Chen, *Chem. Commun.*, 2011, **47**, 9480.

15 C. Kanimozhi, N. Yaacobi-Gross, K. W. Chou, A. Amassian, T. D. Anthopoulos and S. Patil, *J. Am. Chem. Soc.*, 2012, **134**, 16532.

16 J. D. Yuen, J. Fan, J. Seifter, B. Lim, R. Hufschmid, A. J. Heeger and F. Wudl, *J. Am. Chem. Soc.*, 2011, **133**, 20799.

17 H.-W. Lin, W.-Y. Lee and W.-C. Chen, *J. Mater. Chem.*, 2012, **22**, 2120.

18 (a) J. C. Bijleveld, A. P. Zoombelt, S. G. J. Mathijssen, M. M. Wienk, M. Turbiez, D. M. de Leeuw and R. A. J. Janssen, *J. Am. Chem. Soc.*, 2009, **131**, 16616; (b) X. Zhang, L. J. Richter, D. M. DeLongchamp, R. J. Kline, M. R. Hammond, I. McCulloch, M. Heeney, R. S. Ashraf, J. N. Smith, T. D. Anthopoulos, B. Schroeder, Y. H. Geerts, D. A. Fischer and M. F. Toney, *J. Am. Chem. Soc.*, 2011, **133**, 15073.

19 Y. Li, P. Sonar, S. P. Singh, M. S. Soh, M. van Meurs and J. Tan, *J. Am. Chem. Soc.*, 2011, **133**, 2198.

20 J.-H. Tsai, W.-Y. Lee, W.-C. Chen, C.-Y. Yu, G.-W. Hwang and C. Ting, *Chem. Mater.*, 2010, **22**, 3290.

21 I. Kang, H.-J. Yun, D. S. Chung, S.-K. Kwon, and Y.-H. Kim, *J. Am. Chem. Soc.,* 2013, **135**, 14896.

22 J. C. Bijleveld, V. S. Gevaerts, D. D. Nuzzo, M. Turbiez, S. G. J. Mathijssen, D. M. de Leeuw, M. M. Wienk and R. A. J. Janssen, *Adv. Mater.*, 2010, **22**, E242.

23 T. L. Nelson, T. M. Young, J. Liu, S. P. Mishra, J. A. Belot, C. L. Balliet, A. E. Javier, T. Kowalewski and R. D. McCullough, *Adv. Mater.*, 2010, **22**, 4617.

24 E. Zhou, Q. Wei, S. Yamakawa, Y. Zhang, K. Tajima, C. Yang and K. Hashimoto, *Macromolecules*, 2010, **43**, 821.

25 E. Zhou, S. Yamakawa, K. Tajima, C. Yang and K. Hashimoto, *Chem. Mater.*, 2009, **21**, 4055.

26 J. S. Lee, S. K. Son, S. Song, H. Kim, D. R. Lee, K. Kim, M. J. Ko, D. H. Choi, B. Kim and J. H. Cho, *Chem. Mater.*, 2012, **24**, 1316.

27 Y. Li, S. P. Singh and P. Sonar, *Adv. Mater.*, 2010, **22**, 4862.

28 J. S. Ha, K. H. Kim and D. H. Choi, *J. Am. Chem. Soc.*, 2011, **133**, 10364.

29 I. Kang, T. K. An, J. Hong, H.-J. Yun, R. Kim, D. S. Chung, C. E. Park, Y.-H. Kim and S.-K. Kwon, *Adv. Mater.*, 2013, **25**, 524.

30 (a) P. Sonar, S. P. Singh, Y. Li, M. S. Soh and A. Dodabalapur, *Adv. Mater.*, 2010, **22**, 5409; (b) S. Cho, J. Lee, M. Tong, J. H. Seo and C. Yang, *Adv. Funct. Mater.*, 2011, **21**, 1910.

31 M. Al-Hashimi, M. A. Baklar, F. Colleaux, S. E. Watkins, T. D. Anthopoulos, N. Stingelin and M. Heeney, *Macromolecules*, 2011, **44**, 5194.

32 Z. Chen, H. Lemke, S. Albert-Seifried, M. Caironi, M. M. Nielsen, M. Heeney, W. Zhang, I. McCulloch and H. Sirringhaus, *Adv. Mater.*, 2010, **22**, 2371.

33 Y. M. Kim, E. Lim, I.-N. Kang, B.-J. Jung, J. Lee, B. W. Koo, L.-M. Do and H.-K. Shim, *Macromolecules*, 2006, **39**, 4081.

34 (a) M. M. Wienk, M. Turbiez, J. Gilot, R. A. J. Janssen, *Adv. Mater.*, 2008, **20**, 2556; (b) L. Bürgi, M. Turbiez, R. Pfeiffer, F. Bienewald, H.-J. Kirner and C. Winnewisser, *Adv. Mater.*, 2008, **20**, 2217.

35 (a) C. H. Woo, P. M. Beaujuge, T. W. Holcombe, O. P. Lee and J. M. J. Fréchet, *J. Am. Chem. Soc.*, 2010, **132**, 15547; (b) J. C. Biljlevled, B. P. Karsten, S. G. J. Mathijssen, M. M. Wienk, D. M. de Leeuw and R. A. J. Janssen, *J. Mater. Chem.*, 2011, **21**, 1600.

36 (a) H. Bronstein, Z. Chen, R. S. Ashraf, W. Zhang, J. Du, J. R. Durrant, P. S. Tuladhar, K. Song, S. E. Watkins, Y. Geerts, M. M. Wienk, R. A. J. Janssen, T. Anthopoulos, H. Sirringhaus, M. Heeney and I. McCulloch, *J. Am. Chem. Soc.*, 2011, **133**, 3272; (b) I. Meager, R. S. Ashraf, S. Rossbauer, H. Bronstein, J. E. Donaghey, J. Marshall, B. C. Schroeder, M. Heeney, T. D. Anthopoulos and I. McCulloch, *Macromolecules*, 2013, **46**, 5961.

37 B. Tieke, A. R. Rabindranath, K. Zhang and Y. Zhu, *Beilstein J. Org. Chem.* 2010, **6**, 830.

38 Z. Chen, M. J. Lee, R. S. Ashraf, Y. Gu, S. Albert-Seifried, M. M. Nielsen, B. Schroeder, T. D. Anthopoulos, M. Heeney, I. McCulloch and H. Sirringhaus, *Adv. Mater.*, 2012, **24**, 647.

39 (a) M. Shahid, T. McCarthy-Ward, J. Labram, S. Rossbauer, E. B. Domingo, S. E. Watkins, N. Stingelin, T. D. Anthopoulos and M. Heeney, *Chem. Sci.* 2012, **3**, 181; (b) M. Shahid, R. S. Ashraf, Z. Huang, A. J. Kronemeijer, T. McCarthy-Ward, I. McCulloch, J. R. Durrant, H. Sirringhaus and M. Heeney, *J. Mater. Chem.*, 2012, **22**, 12817; (c) A. J. Kronemeijer, E. Gili, M. Shahid, J. Rivnay, A. Salleo, M. Heeney and H. Sirringhaus, *Adv. Mater.*, 2012, **24**, 1558.

40 H. A. Saadeh, L. Lu, F. He, J. E. Bullock, W. Wang, B. Carsten and Y. Yu, *ACS Macro Lett.*, 2012, **1**, 361.

41 B. Lim, K.-J. Baeg, H.-G. Jeong, J. Jo, H. Kim, J.-W. Park, Y.-Y. Noh, D. Vak, J.-H. Park, J.-W. Park and D.-Y. Kim, *Adv. Mater.*, 2009, **21**, 2808.

42 (a) H. Pang, P. J. Skabara, S. Gordeyev, J. J. W. McDouall, S. J. Coles and M. B. Hursthouse, *Chem. Mater.*, 2007, **19**, 301; (b) A. Patra, Y. H. Wijsboom, G. Leitus and M. Bendikov, *Chem. Mater.*, 2011, **23**, 896.

Table of Content